Optical direct-detection OFDM signal generation for radio-over-fiber link using frequency doubling scheme with carrier suppression

Chun-Ting Lin[1*], Yu-Min Lin[2], Jason (Jyehong) Chen[1], Sheng-Peng Dai[1], Po Tsung Shih[1], Peng-Chun Peng[3], and Sien Chi[1,4]

1. Department of photonics and institute of electro-optical engineering, National Chiao-Tung University Hsinchu 300, Taiwan

2. Information and Communications Research Labs, Industrial Technology Research Institute, Hsinchu 300, Taiwan.

3. Department of Applied Materials and Optoelectronic Engineering, National Chi Nan University, Nantou 545 Taiwan.

4. Department of Electrical Engineering, Yuan-Ze University, Chung Li 320, Taiwan

Corresponding Author: jinting@ms94.url.com.tw[*]

Abstract: This investigation demonstrates the generation of OFDM-RoF signal using frequency doubling technique for the first time, to the author's best knowledge. The 4-Gb/s OFDM signal using 16-QAM format modulated on each subcarrier at a center frequency of 19GHz is experimentally demonstrated. Benchmarked against the OOK format, the 16-QAM OFDM format has the higher spectral efficiency with a sensitivity penalty of less than 2.6 dB. After transmission over 50-km single mode fiber, the power penalties of RF OOK and OFDM signals are less than 0.5dB.

OCIS codes: (060.2330) Fiber optics communications; (060.2360) Fiber optics links and subsystems; (060.4370).

References and links

1. J. Lowery and J. Armstrong, "Orthogonal-frequency-division multiplexing for dispersion compensation of long-haul optical systems," Opt. Express **14**, 2079-2084 (2006).
2. B. Djordjevic and B. Vasic, "Orthogonal frequency division multiplexing for high-speed optical transmission," Opt. Express **14**, 3767-3775 (2006).
3. H. Bao and W. Shieh, "Transmission simulation of coherent optical OFDM signals in WDM systems," Opt. Express **15**, 4410-4418 (2007).
4. W. H. Chen, and W. I. Way, "Multichannel Single-Sideband SCM/DWDM Transmission System," J. Lightwave Technol. **22**, 1697-1693 (2004).
5. Wu and X. Zhang, "Impact of Nonlinear Distortion in Radio Over Fiber Systems with Single-Sideband and Tandem Single-Sideband Subcarrier Modulations," J. Lightwave Technol. **24**, 2076-2090 (2006).
6. J. Yu, Z. Jia, L. Yi, G. K. Chang, and T. Wang, "Optical millimeter wave generation or up-conversion using external modulators," IEEE Photon. Technol. Lett. **18**, 265–267 (2006).
7. J. J. O'Reilly, P. M. Lane, R. Heidemann, and R. Hofstetter, "Optical generation of very narrow linewidth millimeter wave signals," Electron. Lett. **28**, 2309–2311 (1992).
8. Lim, C. Lin, M. Attygalle, A. Nirmalathas, D. Novak, and R. Waterhouse, "Analysis of Optical Carrier-to-Sideband Ratio for Improving Transmission Performance in Fiber-Radio Links," IEEE J. Lightwave Technol. **54**, 2181-2187 (2006).
9. L. N. Langey, M. D. Elkin, C. Edge, M. J. Wale, U. Gliese, X. Huang, and A. J. Seeds, "Packaged semiconductor laser optical phase-locked loop (OPLL) for photonic generation, processing and transmission of microwave signals," IEEE Trans. Microwave Theory Technol **47**, 1257-1264 (1999).
10. S. Choi, Y. Shoji, and H. Ogawa, "Millimeter-wave fiber-fed wireless access system based on dense wavelength-division-multiplexing networks," IEEE Trans. Microwave Theory Technol **56**, 232-241 (2008).
11. T. Sakamoto, T. Kawanishi, and M. Izutsu, "Continuous-phase frequency-shift keying with external modulation," IEEE J. Sel. Top. Quantum Electron. **12**, 589–595 (2006).
12. W. Shieh, X. Yi, and Y. Tang, "Experimental Demonstration of Transmission of Coherent Optical OFDM Systems," OFC/NFOEC 2007, OMP2, March, 2007.
13. V. J. Urick, J. X. Qiu, and F. Bucholtz, "Wide-band QAM-over-fiber using phase modulation and

#90231 - $15.00 USD Received 29 Nov 2007; revised 2 Apr 2008; accepted 6 Apr 2008; published 25 Apr 2008

interferometric demodulation," IEEE Photon. Technol. Lett., **16**, 2374-2376 (2004).
14. M. KaveHrad and E. Savov, "Fiber-Optic Transmission of Microwave 64-QAM Signals," IEEE J. Sel. Areas in Commun. **8**, 1320-1326 (1990).

1. Introduction

The combination of orthogonal frequency-division multiplexing (OFDM) and radio-over-fiber (RoF) systems (OFDM-RoF) has attracted considerable attention for future gigabit broadband wireless communication. The high peak to average power ratio (PAPR) and the nonlinear distortion of the optical transmitter are the main issues raised by OFDM and RoF systems [1-5], respectively. The optical radio frequency (RF) signal generation using an external Mach-Zehnder modulator (MZM) based on double-sideband (DSB), single-sideband (SSB), and double-sideband with optical carrier suppression (DSBCS) modulation schemes have been demonstrated [1,2,4-8]. Since the optical RF signals are weakly modulated because of the narrow linear region of MZM, those that have undergone DSB and SSB modulation suffer from inferior sensitivities due to limited optical modulation index (OMI) [4-6,8]. Hence, an optical filter is needed to improve the performance [8]. Furthermore, the DSB signal experiences the problem of performance fading because of fiber dispersion [6]. Among these modulation schemes, DSBCS modulation has been demonstrated to be effective in the millimeter-wave range with excellent spectral efficiency, a low bandwidth requirement for electrical components, and superior receiver sensitivity following transmission over a long distance [6]. However, all of the proposed DSBCS schemes can only support on-off keying (OOK) format, and none can transmit vector modulation formats, such as phase shift keying (PSK), quadrature amplitude modulation (QAM), or OFDM signals, which are of utmost importance for wireless applications.

On the other hand, optical RF signal generations using remote heterodyne detection (RHD) have been also demonstrated [9-10]. The advantage of RHD systems is that the vector signal can be modulated at baseband. Therefore, the bandwidth requirement of the transmitter is low. However, the drawback is that phase noise and wavelength stability of the lasers at both transmitter and receiver should be carefully controlled.

This study proposes a novel method for generating optical direct-detection OFDM-RoF signals using a new DSBCS modulation scheme that can carry vector signals. A frequency doubling scheme is employed to reduce the requirement of bandwidth of electronic components, which is an important issue at millimeter-wave RoF systems. Benchmarked against the OOK format, the 4-Gb/s 16-QAM OFDM format has the higher spectral efficiency with a sensitivity penalty of under 2.6-dB.

2. Concept of proposed system

Figure 1 schematically depicts the principle of the proposed optical direct-detection OFDM-RoF signal generation. An integrated x-cut $LiNbO_3$ MZM [11], comprising three single-electrode MZMs, is key to generating optical RF signals. Two sub-MZMs (MZ-a and MZ-b) are embedded in each arm of the main modulator (MZ-c). When both MZ-a and MZ-b are biased at the null point, the generated optical spectrum consists of an upper sideband (USB) and a lower sideband (LSB) with optical carrier suppression. Except with a phase difference of 90°, the RF signals sent into the MZ-a and MZ-b are exactly the same. When MZ-c is biased at the quadrature point, either USB or LSB will be eliminated at the output of the integrated MZM.

The basic operation principle is as follow. When MZ-a and MZ-b are biased at the null point, only odd-order optical sidebands will be generated. To simplify the concept, only two first-order sidebands (USB and LSB) are shown in the optical spectrum insets of Fig. 1. Firstly, for the data path, the inset (i) shows the generated USB and LSB at the output of MZ-a.

#90231 - $15.00 USD Received 29 Nov 2007; revised 2 Apr 2008; accepted 6 Apr 2008; published 25 Apr 2008

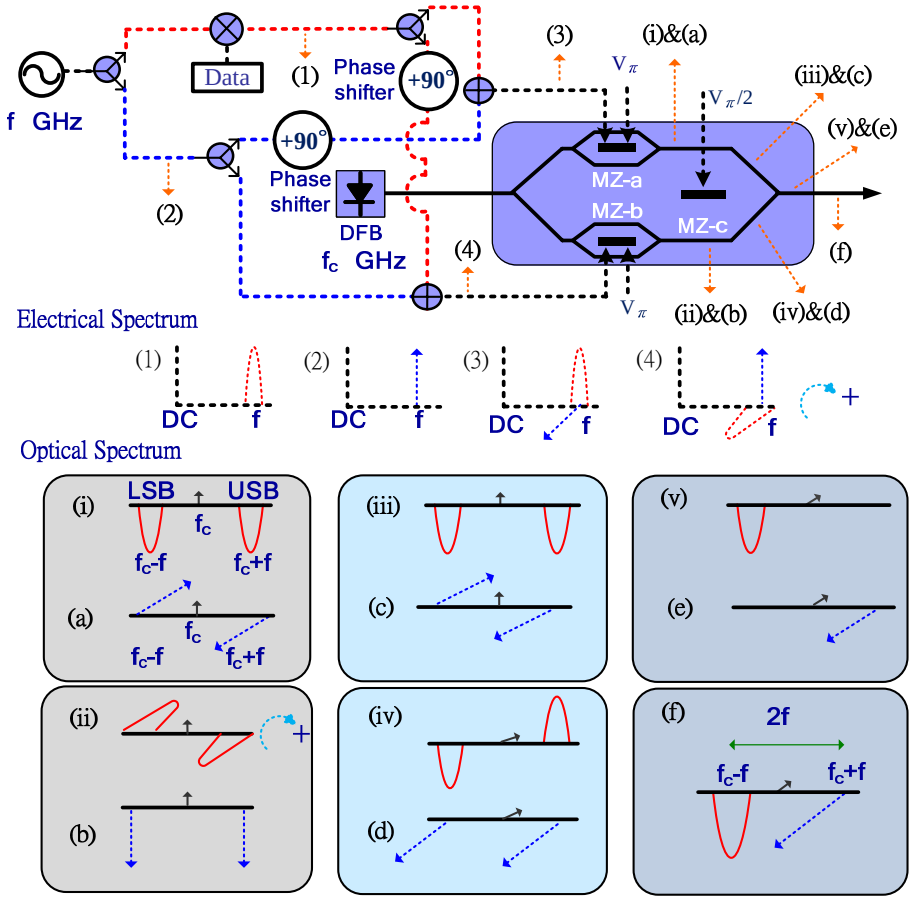

Fig. 1. Conceptual diagram of generating direct-detection optical OFDM-RoF signals. (1)(2)(3)(4): Electrical input signal. (i)(ii)(ii)(iv)(v): Optical spectrum of data signal. (a)(b)(c)(d)(e): Optical spectrum of sinusoidal signal. (f): Optical spectrum of RF signal.

Because a 90° phase shift is added at MZ-b, the generated USB and LSB need to rotate +90° and -90°, respectively, as shown in inset (ii). Biasing MZ-c at the quadrature point will add another +90° phase shift for all optical sidebands from MZ-b, as shown in inset (iv). After combination of insets (iii) and (iv), an optical single sideband (LSB) with carrier suppression is obtained as shown in inset (v). The operation principle of the sinusoidal signal path is similar and is shown in inset (a) to (d).Therefore, as both sinusoidal and data-modulated signals are simultaneously sent to integrated MZM, as shown in insets (3) and (4) of Fig.1, the optical generated signal consisting of the two-tone lightwave, which can be converted into electrical RF signals by square-law photo-diode (PD) detection, can be produced at the output of the transmitter.

Since the RF signal can be modulated only at either the USB or the LSB, the proposed system can generate not only OOK signals but also PSK, QAM and OFDM signals. Additionally, the relative intensity between USB and LSB can be easily tuned by adjusting the individual power of the electrical sinusoidal and data signals to optimize the performance of the optical RF signals. A frequency doubling approach is employed to reduce the cost of the electronic components, especially for the RF signal in the millimeter-wave range.

3. Experimental results and discussions

Figure 2 depicts the experimental setup. Both RF OFDM and OOK signals are demonstrated in our proposed architecture. The block diagram of the typical OFDM transmitter is shown in

#90231 - $15.00 USD Received 29 Nov 2007; revised 2 Apr 2008; accepted 6 Apr 2008; published 25 Apr 2008

Fig. 3(a). The OFDM signal is generated using a 4GHz arbitrary waveform generator (AWG) with eight carriers, and each subcarrier is encoded with 62.5MHz 16-QAM symbol, as shown in Fig. 4(a). The cyclic prefix is 1/32 symbol time. The OFDM signal is up-converted to 9.5GHz by a mixer, as shown in Fig. 4(b). Since the

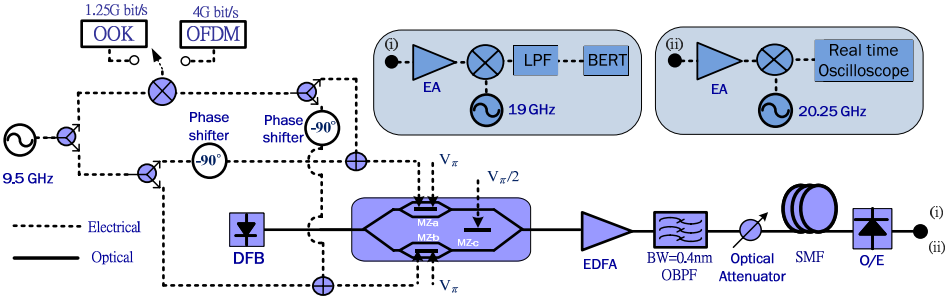

Fig. 2. Experimental setup of optical RF signal generation and (i) RF OOK and (ii) RF OFDM signal receivers. (V_π: half-wave voltage of MZM. EA: electrical amplifier. EDFA: Erbium-doped optical fiber amplifier, LPF: low-pass filter. OBPF: optical band-pass filter. SMF: single mode fiber. O/E: optical to electrical conversion)

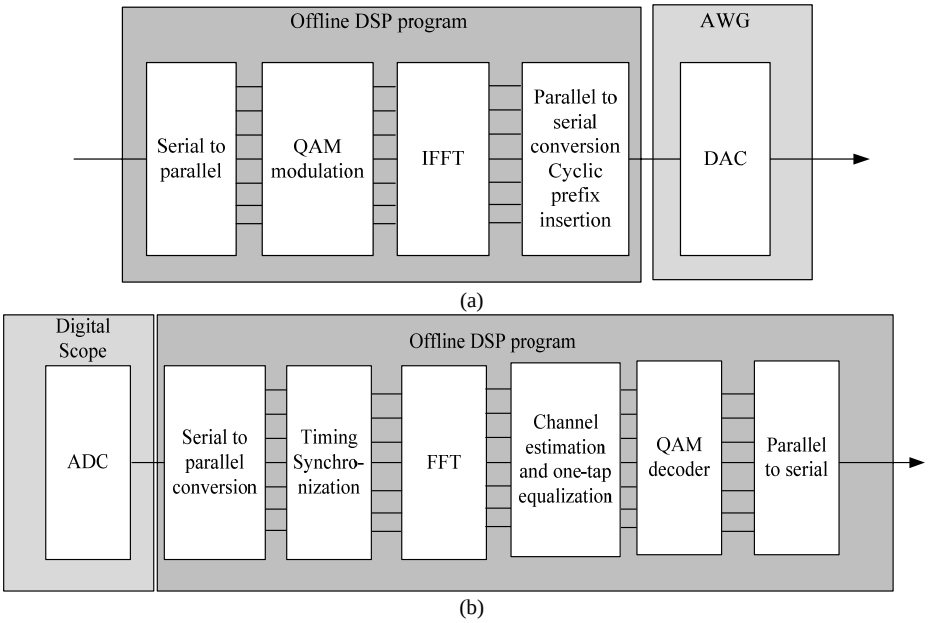

Fig. 3. Block diagrams of OFDM transmitter (a) and receiver (b). (IFFT: inverse fast Fourier transform, DAC: digital to analog converter, ADC: analog to digital converter, FFT: fast Fourier transform).

AWG has only one output, the lower sideband and upper sideband of the electrical OFDM signal are not mutually independent. Notably, the constraint between the subcarriers' symbols has negligible effect on the system performance because every subcarrier is demodulated independently [12]. Therefore, with such a setup, a 4-Gb/s RF OFDM signal that has 16 subcarriers and occupies a total bandwidth of 1GHz can be generated at a center frequency of 9.5GHz. The OOK baseband signal with a pseudo random binary sequence (PRBS) of word length of 2^{31}-1 is generated by a pattern generator and then pass through a low-pass filter with a 3-dB bandwidth of 1 GHz. The OOK signal is up-converted to a center frequency of 9.5

#90231 - $15.00 USD Received 29 Nov 2007; revised 2 Apr 2008; accepted 6 Apr 2008; published 25 Apr 2008

GHz and the bandwidth of the up-converted OOK signal is around 2 GHz.

The RF OFDM/OOK signal at 9.5GHz is then split using a 90° hybrid coupler to drive MZ-a and MZ-b. Figure 5(b) shows that the OFDM signal is modulated on the optical LSB. The same mechanism is used to split the 9.5GHz sinusoidal signal to drive MZ-a and MZ-b. Figure 5(a) reveals that a new optical carrier can be generated at the USB of the original carrier by 9.5GHz. Figure 5(c) presents the optical RF OFDM spectrum when both signals are turned on. Notably, the distance between the OFDM signal and the new optical carrier is 19GHz. The optical spectra of OOK and RF OOK signals are also shown in Figs. 5(d) and 5(e), respectively. Note that the optical carrier suppression ratio and the undesired sideband suppress ratio of both RF OFDM and OOK signals are greater than

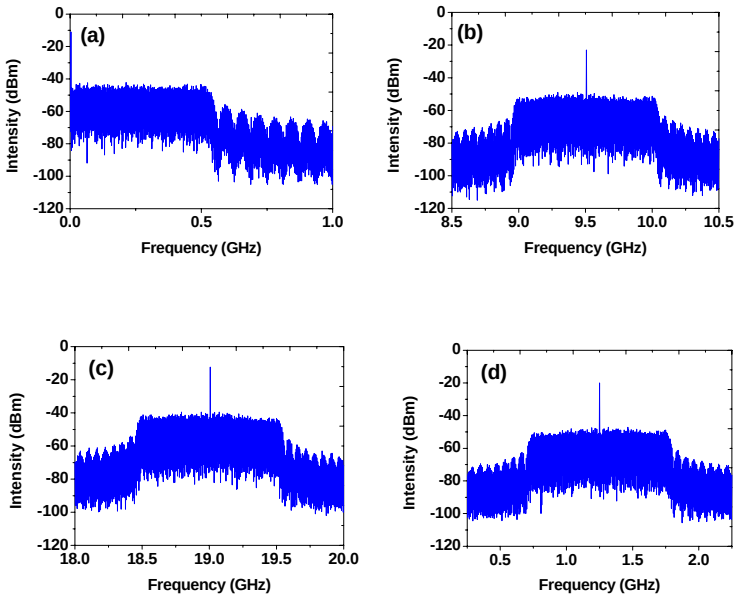

Fig. 4. Electrical spectra of OFDM signals. (a) After AWG. (b) After up-conversion. (c) After PD detection. (d) After down-conversion.

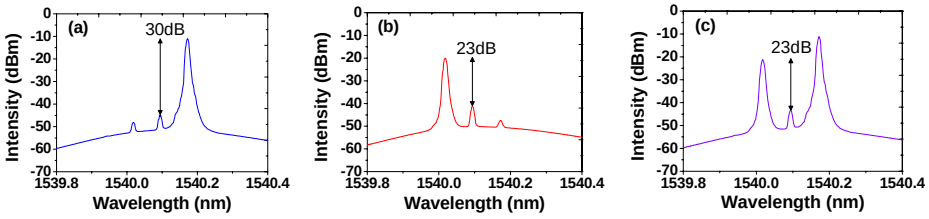

#90231 - $15.00 USD Received 29 Nov 2007; revised 2 Apr 2008; accepted 6 Apr 2008; published 25 Apr 2008

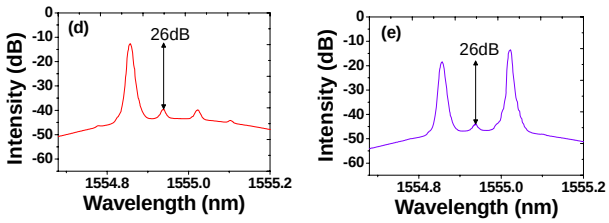

Fig. 5. Optical spectra of RF signals. (a) Sinusoidal signal. (b) OFDM signal. (c) RF OFDM signal. (d) OOK signal. (e) RF OOK signal.

23dB, which has a negligible influence on the performance of the generated RF signals. The generated RF signal is then amplified by using an Erbium-doped Optical Fiber Amplifier (EDFA) and filtered through a 0.4-nm optical filter to suppress the ASE noise. Then, an optical attenuator is used to set the optical launched power to 0 dBm before transmission to prevent fiber nonlinearity. The 25-km or 50-km single mode fiber (SMF) is used to evaluate the transmission penalty of the system.

Insets (i) and (ii) of Fig. 2 display the receiver architectures of RF OOK and OFDM signals, respectively. The electrical RF OFDM signal is centered at 19 GHz after O/E conversion, as shown in Fig. 4(c). In RoF applications, this signal can be directly utilized for wireless transmission. Since the bandwidth of our digital real-time oscilloscope is 4GHz, the OFDM signal is down-converted to 1.25GHz by a 20.25GHz oscillator and a mixer to realize intermediate frequency (IF) demodulation. Figure 4(d) depicts the IF signal spectrum. A 20-GHz real-time oscilloscope stores the waveform and the off-line

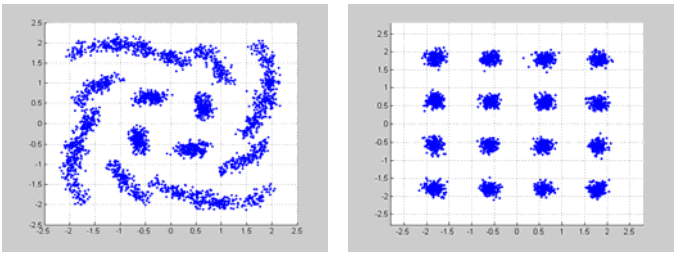

(a) (b)

#90231 - $15.00 USD Received 29 Nov 2007; revised 2 Apr 2008; accepted 6 Apr 2008; published 25 Apr 2008

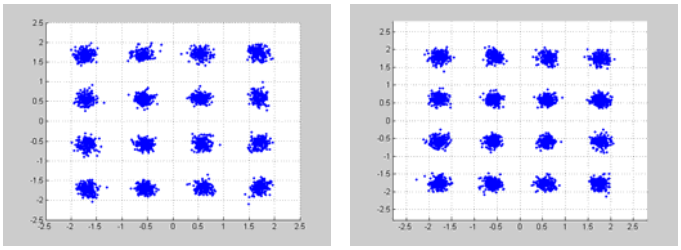

(c) (d)

Fig. 6. Constellations of OFDM signal with optical power of -13dBm. (a) BTB before equalization. (b) BTB after equalization. (c) After transmission over 25km SMF. (d) After transmission over 50km SMF.

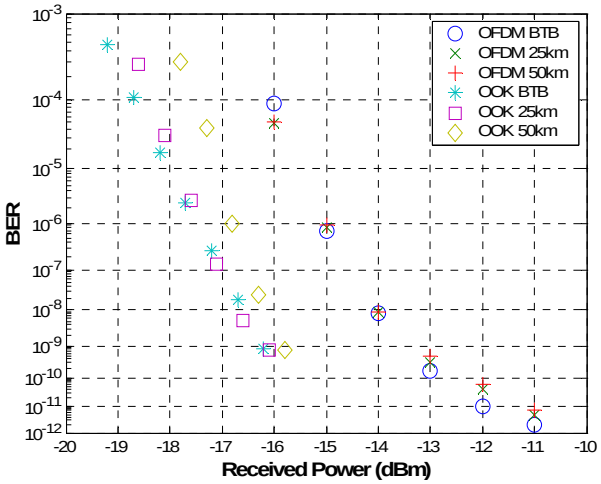

Fig. 7. BER curves of RF OFDM and OOK signals.

digital signal processing (DSP) program is employed to demodulate the OFDM signal. The block diagram of the OFDM receiver is shown in Fig. 3(b). The demodulation process includes synchronization, Fast Fourier Transform (FFT), one-tap equalization, and QAM symbol decoding. The bit error rate (BER) performance is calculated from the measured error vector magnitude (EVM) [13-14]. The 1.25-Gb/s OOK signal at 19GHz is also tested in the proposed architecture but is down-converted to baseband signal. Then, the OOK baseband signal is directly tested by the BER tester without the off-line DSP program.

Figures 6(a) and 6(b) show 16QAM constellation diagrams before and after the one-tap equalizer in back to back (BTB) case, respectively. The equalizer in OFDM transceiver is used to combat both frequency response of various microwave components and fiber dispersion. Figures 6(c) and 6(d) present the 16-QAM constellation diagrams after 25-km and 50-km SMF transmission, respectively. With the QAM's high bandwidth utilization efficiency, the 4-Gb/s data only occupies 1GHz bandwidth and fiber chromatic dispersion effect is negligible. Figure 7 shows the BER performance. For OFDM signals, the receiver sensitivity of 13.4dBm was achieved at a BER of 10^{-9} in the BTB case. The penalty at a BER of 10^{-9} is less than 0.2 dB following 25-km or 50-km SMF transmission. The performance of OOK signals is 2.6 dB better than that of OFDM signals at the cost of lower bandwidth efficiency.

#90231 - $15.00 USD Received 29 Nov 2007; revised 2 Apr 2008; accepted 6 Apr 2008; published 25 Apr 2008

4. Conclusions

It is of utmost important for the RoF system to support such vector signals that have been widely used in wireless communication. The OFDM format is particularly attractive due to its resistance to multi-path fading. The proposed architecture utilizes the carrier suppression technique to achieve frequency doubling and successfully transmits a high capacity 4-Gb/s OFDM signal over 50 km SMF with negligible sensitivity penalty.

Acknowledgment

The authors would like to thank the National Science Council of the Republic of China, Taiwan, for financially supporting this research under Contract Nos. NSC 96-2221-E-155-038-MY2, NSC 96-2752-E-009-004-PAE, NSC 96-2628-E-009-016, and NSC 95-2112-M-260-001-MY2.

#90231 - $15.00 USD Received 29 Nov 2007; revised 2 Apr 2008; accepted 6 Apr 2008; published 25 Apr 2008